Analytical and Bioanalytical Chemistry (2021) 413:6941–6949
https://doi.org/10.1007/s00216-021-03662-4

PAPER IN FOREFRONT

Portable, quantitative, and sequential monitoring of copper ions and pyrophosphate based on a DNAzyme-Fe_3O_4 nanosystem and glucometer readout

Chunchuan Gu[1] · Xiang Chen[2] · Hongying Liu[3]

Received: 21 June 2021 / Revised: 1 September 2021 / Accepted: 13 September 2021 / Published online: 1 October 2021

Abstract

In this report, portable, quantitative, and sequential monitoring of copper ions and pyrophosphate (PPi) with a single sensor based on a DNAzyme-Fe_3O_4 system and glucometer readout was performed. Initially, streptavidin was functionalized on the surface of magnetic Fe_3O_4 spheres through glutaraldehyde. Then, an invertase-modified DNA Cu substrate was connected to the magnetic Fe_3O_4 spheres by a specific reaction between streptavidin and biotin. The sensing system was formed by a hybridization reaction between the Cu substrate and Cu enzyme. In the presence of Cu^{2+}, Cu^{2+} will recognize the Cu DNA substrate and form an "off-on" signal switch, thereby resulting in the separation of invertase from the Fe_3O_4 nanospheres. PPi recognizes Cu^{2+} to form a Cu^{2+}-PPi complex, resulting in an "on-off" signal switch. Under optimized conditions, linear detection ranges for Cu^{2+} and PPi of 0.01–5 and 0.5–10 μM, and detection limits for Cu^{2+} and PPi of 10 nM and 500 nM, respectively, were obtained. Good selectivity was achieved for the analysis of Cu^{2+} and PPi. Satisfactory results were achieved for this biosensor during the determination of Cu^{2+} in real tap samples and PPi in human urine samples. This verified that the sensor is portable and low cost, and can be applied to the sequential monitoring of multiple analytes with a single point-of-care biosensor.

Keywords Personal glucose meter · Copper ion · Pyrophosphate ion · Biosensor · Fe_3O_4 nanoparticles · Sequential monitoring · DNAzyme

Introduction

Copper ions (Cu^{2+}), an essential heavy metal element for living organisms, are widely involved in a series of processes in biological systems, such as electron transfer and redox reactions. They play very significant roles as a catalytic cofactor in different cellular physiological processes [1]. A lack of copper in organisms can lead to growth and metabolic disorders, while excessive copper can also produce toxic effects. For example, neurodegenerative diseases including Parkinson's, Myankos, Wilson's, Alzheimer's, and amyotrophic lateral sclerosis are caused by the disruption of copper metabolism balance in vivo [2]. Pyrophosphate ions (PPi, $P_2O_7^{4-}$), as the major anions in biological systems, are produced during DNA polymerization, enzymatic reactions, and cellular metabolism [3]. Published reports suggest that abnormal concentrations of PPi in living cells can cause some diseases, such as arthritis and chondrocalcinosis [4]. Driven by the great significance of Cu^{2+} and PPi, substantial efforts have been made and various strategies including electrochemistry [5], colorimetry [6], surface-enhanced Raman spectroscopy (SERS) [7], surface plasmon resonance (SPR) [8], and fluorescence [9] have been adopted. These methods supply effective and diverse approaches for the determination of Cu^{2+} and PPi in a large variety of cases. For example, Wang et al. have reported several fluorescent biosensors for the determination of heavy ions and PPi with a low detection limit and wide linear range [10–13]. However, some inevitable limitations, such as

✉ Xiang Chen
123269799@qq.com

✉ Hongying Liu
liuhongying@hdu.edu.cn

[1] Department of Clinical Laboratory, Hangzhou Cancer Hospital, Hangzhou 310002, Zhejiang, China

[2] Department of Biomedical Sciences Laboratory, Affiliated Dongyang Hospital of Wenzhou Medical University, Dongyang 322100, Zhejiang, China

[3] College of Automation, Hangzhou Dianzi University, Hangzhou 310018, Zhejiang, China

expensive instruments and sophisticated operating procedures remain. To tackle this problem, it is of significance to develop new methods that are low cost and portable.

Point-of-care testing (POCT) involves clinical and bedside tests performed at the bedside of a patient. It has attracted increasing attention because it is portable, low cost, user friendly, and on site [14, 15]. The most comprehensive POCT involves the use of a personal glucose meter (PGM), which is widely used by diabetes patients to monitor blood glucose levels at home [16]. It allows the values of the glucose concentration in the patient's body to be read off easily through a drop of blood. Consequently, it has raised the quality of life for millions of diabetic patients from all four corners of the world. However, it usually detects only one object, glucose. To make use of a PGM with many comparable advantages for other targets, Lu et al. reported the first example of utilizing a PGM to detect nonglucose targets [17]. To date, various targets, including proteins [18], nucleic acids [19, 20], enzyme activity [21], SARS-CoV-2 [22], foodborne pathogenic bacteria [23], ochratoxin A [24], pesticides and veterinary drug residues [25], and heavy metal ions [26], have been detected by PGM. We have also summarized the application of a blood glucose meter from three aspects: biomedical analysis, food analysis, and environmental analysis [27]. However, there are only two articles in the literature about Cu^{2+} detection based on a PGM. In 2014, Xiang et al. developed a Cu^{2+}-sensing system based on an invertase-modified magnetic bead signal amplification probe and a PGM [28]. In 2017, aided by a ligation DNAzyme releasing strategy and a PGM, Lv et al. developed a portable and sensitive Cu^{2+}-sensing system [29]. To our knowledge, PGM-based sensors for selective Cu^{2+} and PPi have not been reported to date. Usually, multiple analytes are often limited by tedious sampling and time-consuming pretreatments. Sequential detection with a single sensor has attracted increasing attention due to its low cost, fast speed, and effective analysis.

Inspired by the above considerations, we first report a novel sequential detection of Cu^{2+} and PPi with a single sensor based on the use of a PGM as a readout tool and a magnetic sphere as the separation tool. The designed strategy is shown in Scheme 1. Magnetic Fe_3O_4 spheres are prepared by the hydrothermal method, and then capped with SiO_2. After functionalization with streptavidin, invertase was modified with a DNA-named Cu substrate and Cu DNA enzyme to form a sensing system. Upon targeting Cu^{2+}, Cu^{2+} will recognize the Cu DNA substrate and form an "on-off" signal switch, thereby resulting in the separation of invertase from the Fe_3O_4 nanospheres. In the presence of PPi, PPi will recognize Cu^{2+} to form a Cu^{2+}-PPi complex, resulting in an "off-on" signal switch. This signal change was collected by a portable PGM. Therefore, a cost-effectiveness and portable biosensor for the consecutive detection of Cu^{2+} and PPi was built on the basis of the above "on-off-on" system. This biosensor will provide potential applications in the fields of molecular diagnosis and environmental monitoring.

Experimental

Reagents

We purchased $FeCl_3.6H_2O$ and sucrose from Sangon Biotech Co., Ltd. (China). $CH_3COONa.3H_2O$, ammonia, ethylene glycol, tetraethylorthosilane (TEOS), and 3-aminopropyl) triethoxysilane (APTES) were provided by Aladdin Industrial Co., Ltd. (China). 4-(N-Maleimidomethyl) cyclohexane-1-carboxylic acid 3-sulfo-N-hydroxysuccinimide ester sodium salt (sulfo-SMCC), 1-(3-(dimethylamino)-propyl)-3-ethylcarbodiimide hydrochloride (EDC), N-hydroxysulfosuccinimide sodium salt (sulfo-NHS), invertase (β-fructose-dase, from Baker's yeast), Tris (2-car-boxyethyl) phosphine hydrochloride (TCEP), and Tween-20 were obtained from Sigma-Aldrich Co., Ltd. (USA). Reagents used in the polyacrylamide gel electrophoresis experiment and DNA sequences were provided by Sangon Biotechnology Co., Ltd. (Shanghai, China). The laboratory water was deionized water (≥ 18 MΩ·cm, Millipore).

Other buffer solutions were also employed:

Buffer A: 0.1 M sodium phosphate buffer including 0.1 M NaCl (pH 7.4)
Buffer B: 0.1 M sodium phosphate buffer including 0.1 M NaCl and 0.05% Tween-20 (pH 7.4)
Buffer C: 0.05 M HEPES including 1.5 M NaCl (pH 7.0)

The DNA sequences used are shown below:

Cu-Enz (5′-GGTAAGCCTGGGCCTCTTTCTTTTTA AGAAAGAAC-3′)
Cu-Sub (5′-biotin-$(A)_9$AGCTTCTTTCTAATACGGCT TACC-$(A)_9(CH_2)_6$SH-3′

Instruments

Field emission scanning electron microscopy (FESEM) and transmission electron microscopy (TEM) images were collected using a JSM-7500 field emission electron microscope and a Tecai G2 F20 S-TWIN (FEI, America) electron microscope. Fourier-transform infrared (FTIR) spectra were measured using a Nicolet Nexus FTIR 670 spectrometer (Thermo, USA) with a measurement range of 400~4000 cm^{-1}. X-ray diffraction (XRD) patterns were measured using a MinFlex 600 X-ray diffractometer. The ultraviolet visible absorption spectrum was measured using a UV-2600 ultraviolet spectrophotometer (Shimadzu, Kyoto, Japan) or a Nanodrop One

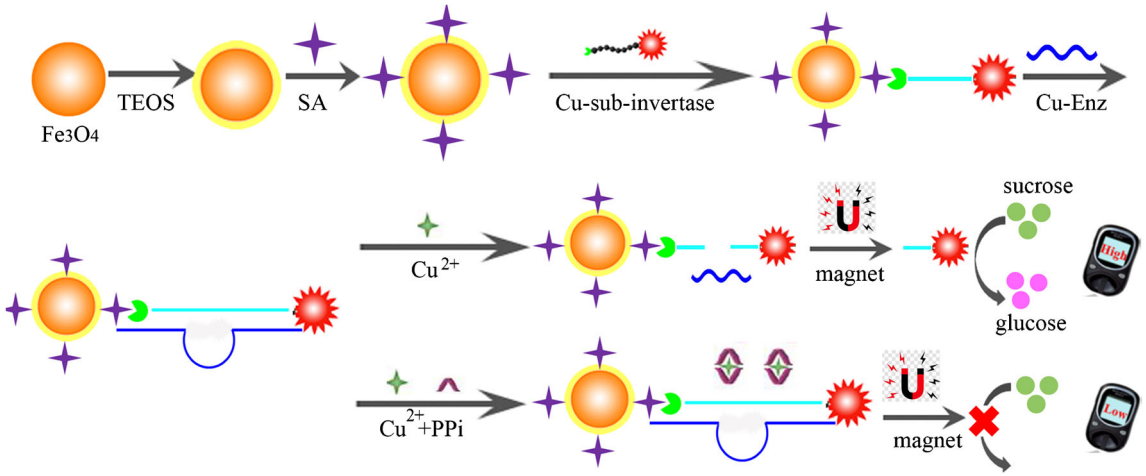

Scheme 1 Schematic illustration for portable and quantitative monitoring of pyrophosphatase activity using DNAzyme with a personal glucose meter

(Thermo Fisher Scientific, America). A glucose meter (ACCU-CHEK Active, Germany) was used to determine the glucose concentration.

Synthesis of Fe_3O_4-NH_2 nanoparticles

The synthesis method for Fe_3O_4 nanoparticles was performed according to the alcohol-thermal method reported in the literature and was appropriately modified [30]. Specifically, $FeCl_3 \cdot 6H_2O$ (1.35 g) was dissolved in ethylene glycol (40 ml) with constant stirring to form a transparent solution. Then, 3.6 g NaAc and 1.0 g polyethylene glycol were added to the above solution. After stirring vigorously for 1 h, the above mixture was placed into a Teflon-lined stainless-steel autoclave and heated for 8 h at 200 °C. A cooling method was used to cool the films from the furnace temperature to room temperature. The precipitate was washed three times with ultrapure ethanol and water. The product was dried for 6 h at a temperature of 60 °C.

Next, 0.04 g Fe_3O_4 was placed in 20 ml ethanol and ultrasonically dispersed for 1 h. Then, 12 ml of ultrapure water and 2 ml of ammonia solution were poured into the solution as described above and transferred into a three-neck flask, and the flask was mechanically stirred in a water bath at 45 °C. Meanwhile, 400 μl TEOS was dissolved in 20 ml ethanol, with mechanical stirring for 10 min. Subsequently, the above mixture was poured into a three-neck flask and mechanically stirred for 6 h. The precipitate was washed three times with ultrapure ethanol and water. The Fe_3O_4-SiO_2 product was dried for 6 h at a temperature of 60 °C.

Third, the obtained Fe_3O_4-SiO_2 was added to 100 ml ethanol (98%, v/v) and mechanically stirred for 20 min. After 100 μl APTES was added, the solution as described above was mechanically stirred for 6 h. Then, the Fe_3O_4-NH_2 nanoparticles were washed three times with ultrapure ethanol and water and dried for 6 h at a temperature of 60 °C.

Synthesis of Fe_3O_4-SA

Streptavidin was coupled to Fe_3O_4-NH_2 nanoparticles by glutaraldehyde. Typically, 5 mg Fe_3O_4-NH_2 nanoparticles were placed in buffer A (5 ml). After ultrasonication for 20 min, 200 μl glutaraldehyde (25%) was added and gently vortexed at 37 °C for 3 h. Subsequently, the solution as described above was washed with PBS four times and suspended in 4.5 ml PBS. After 1 mg/ml streptavidin (100 μg/ml) was added, the solution described above was gently vortexed at 37 °C for 12 h and then finally washed with buffer A.

Synthesis of the Cu sub-invertase

DNA-invertase was synthesized according to the literature procedures [17]. In brief, 0.5 mg sulfo-SMCC was mixed with 100 μl invertase (20 mg/ml) and then vortexed at room temperature for 2 h. Subsequently, excess insoluble sulfo-SMCC was removed by centrifugation (3000 rpm/min, 10 min). The supernatant was then subjected to ultrafiltration with a 100-kDa MW filter and termed solution A. Meanwhile, 60 μl Cu-Sub (20 μM) and 2 μl TCEP (3 mM) were added to 2 μl PBS (0.1 M, pH 5.5). After reacting at room temperature for 1 h, the solution described above was washed with a 30-kDa-MW filter by buffer A and termed solution B. Finally, solutions A and B were mixed and then reacted at room temperature for 48 h. After the solution was purified with a 100-kDa-MW filter using buffer A, the mixture was kept in 100 μl buffer A.

Synthesis of Cu-Sub-Fe_3O_4

Cu sub-invertase was added to the streptavidin-modified Fe_3O_4 solution (5 μM of the final concentration). After the solution was mixed gently at room temperature for 0.5 h, the Cu-Sub-Fe_3O_4 was washed with buffer A three times with a magnet.

Detection of Cu^{2+}

First, Cu-Sub-Fe_3O_4 (1 μM), Cu-Enz (2 μM), 5 μl of 5 mM ascorbate, and various concentrations of Cu^{2+} were added to 200 μl buffer C for 2 h at 43 °C to form a sensing system. Then, the above system was washed with a magnet to remove the excess Cu-Enz. Subsequently, 5 μl sucrose (1 M) was added to the 10-μl sensing system. After reacting at room temperature for 40 min, a PGM was used to measure the glucose concentration.

Detection of PPi

First, 1 μM Cu-Sub-Fe_3O_4, 2 μM Cu-Enz, 5 μl of 5 mM ascorbate, Cu^{2+} (5 μM), and various concentrations of PPi were added to 200 μl buffer C for 3 h at 43 °C to form a sensing system. Then, we removed the excess Cu-Enz from the above system with a magnet. Afterwards, 5 μl sucrose (1 M) was added to the 10-μl sensing system. After reacting at room temperature for 40 min, a PGM was used to measure the glucose concentration.

Results and discussion

The principle of the fabricated biosensor

The framework of the fabricated biosensor for the determination of Cu^{2+} and PPi is schematically described in Scheme 1. It involves six principal processes: (1) synthesis of magnetic Fe_3O_4@SiO_2 nanoparticles, (2) preparation of Cu-sub-invertase, (3) connection of Cu-sub-invertase with magnetic Fe_3O_4@SiO_2 nanoparticles, (4) formation of the magnetic sensing probe, (5) fabrication of an "off-on" sensing system and PGM detection, and (6) fabrication of an "on-off" sensing system and PGM detection. In step 1, magnetic Fe_3O_4@SiO_2 nanoparticles are first synthesized by the hydrothermal method and then modified with a SiO_2 shell. In step 2, the above magnetic Fe_3O_4 nanoparticles are modified with streptavidin by glutaraldehyde. In step 3, magnetic Fe_3O_4@SiO_2 nanoparticles are connected with DNA through the specific reaction between streptavidin and biotin. In step 4, magnetic sensing probes are fabricated by the hybridization reaction between Cu-EnZ and Cu-sub. After magnetic separation, sucrose is added to the above system to prompt sucrose into glucose, and then the glucose signal is detected by a PGM. At this time, the glucose signal is very low. In step 5, with the existence of Cu^{2+}, it can cut DNA Cu-sub. After magnetic separation, invertase left the magnetic nanoparticles and stayed in the sensing system to prompt sucrose into glucose, and then the glucose signal was detected by a PGM. This will catalyze the conversion of sucrose into glucose and thus obtain a high signal. This is an "off-on" sensing system. Subsequently, with the existence of PPi, a Cu^{2+}-PPi complex was formed by the binding reaction between Cu^{2+} and PPi. After magnetic separation, invertase remained in the system, and thus, a low signal was obtained. This is an "on-off" sensing system. Through the use of this "off-on-off" sensing system, Cu^{2+} and PPi were detected consecutively with one sensor.

Characterization of Fe_3O_4-NH_2 nanoparticles

To realize our design, the most basic precondition for the successful fabrication of DNAzyme-Fe_3O_4 nanosystems is to gain a highly efficient magnetic probe. TEM, XRD, and FTIR were carried out to characterize the morphology of Fe_3O_4-NH_2 nanoparticles. As shown in Fig. 1A, Fe_3O_4 nanoparticles have a better dispersion, particle size uniformity, and homogeneous spherical structure. Compared with bare Fe_3O_4 nanoparticles, a white silicon shell was discovered outside the black Fe_3O_4 nanosphere, indicating the successful preparation of Fe_3O_4@SiO_2 nanospheres. Figure 2B gives the XRD pattern for Fe_3O_4 nanoparticles. Eight sharp diffraction peaks are observed located at 2θ = 30.1°, 35.6°, 37.1°, 43.1°, 53.4°, 56.99°, and 62.6°, which belong to the (220), (311), (222), (400), (422), (511), (440), and (533) crystal planes of the cubic spinel structures for Fe_3O_4 nanoparticles, respectively, from a comparison with JCPDS file Card No. 99-0073. This is consistent with the previous reported literature [31], indicating that Fe_3O_4 nanoparticles were successfully synthesized using this method. Finally, FTIR spectra for Fe_3O_4, Fe_3O_4-SiO_2, and Fe_3O_4-NH_2 were studied and are shown in Fig. 1C. Compared with line a, line b and line c show a new absorbance at 789 cm^{-1} and 1110 cm^{-1}, respectively, corresponding to the plane stretching vibration peaks and bending vibration absorption kurtosis of Si–O–Si, indicating successful preparation of the SiO_2 shell. The stretching vibration peak for N–H at 1612 cm^{-1} was discovered at line c, indicating that the amino groups were successfully connected to the surface of SiO_2-coated magnetic particles [32].

Characterization of the Fe_3O_4-DNA nanocomposite

To achieve our design, the key process for the successful fabrication of DNAzyme-Fe_3O_4 nanosystems is to connect DNA Cu-Enz with Fe_3O_4 nanoparticles. To certify the successful preparation of the magnetic sensing probe, UV-Vis absorbance spectroscopy was conducted for Fe_3O_4@SiO_2 and Fe_3O_4-DNA, as demonstrated in Fig. 2A. A stark absorption peak located at 260 nm is equivalent to that for DNA that appeared for Fe_3O_4@SiO_2 after modification of DNA. In addition, these results also demonstrate the successful synthesis of Fe_3O_4@SiO_2-DNA.

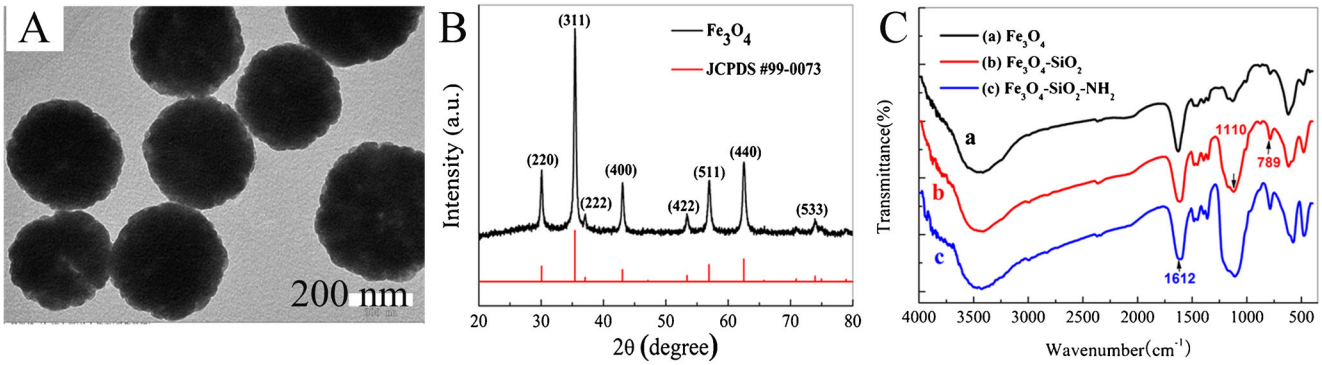

Fig. 1 **A** TEM of Fe_3O_4@SiO_2 and **B** XRD of Fe_3O_4, and **C** FTIR of Fe_3O_4, Fe_3O_4-SiO_2, and Fe_3O_4-NH_2

The feasibility of the fabricated biosensor

A series of control experiments were performed and the PGM readings were collected to demonstrate the feasibility of the fabricated biosensor. As demonstrated in Fig. 2B, the PGM signals for buffer solution (histogram a), Fe_3O_4-DNA (histogram b), and the magnetic sensing probe (histogram c) were low due to no obvious glucose production, indicating that this biosensor has a low background signal. However, in the presence of Cu^{2+}, a much higher signal was generated (histogram d). This indicated that the invertase was introduced into the magnetic sensing probe with the addition of Cu^{2+} because Cu^{2+} could cut Cu-Enz DNA and release the invertase into the sensing system to form an "off-on" sensing system. The generated invertase will catalyze sucrose conversion into glucose, and thus, signals can be captured by a PGM. Subsequently, with the addition of PPi and Cu^{2+}, a lower signal was detected (histogram f). This is because Cu^{2+} is captured by PPi and then the magnetic sensing probe is finally restored shortly to form an "on-off" system. Invertase was removed with the magnetic sensing probe. No amount of glucose was generated, and the signal was very small. This result indicated the feasibility of the designed magnetic sensing probe for sequential detection of Cu^{2+} and PPi.

Optimization of the experimental conditions

For the purpose of realizing the best sensing performance, several experimental parameters for the designed magnetic sensing probe and the detection procedures were optimized. First, the preparation of a magnetic sensing probe was the key step for sequential detection of Cu^{2+} and PPi. Thus, the Cu-sub to Cu-Enz ratio was investigated and is demonstrated in Fig. 3A. As the ratio increased, the PGM signal increased and then reached a plateau after 2:1. This indicated that a ratio of 2:1 is sufficient for the formation of the sensing system, and this value was thus chosen for the optimized condition. Subsequently, the cleavage time for Cu^{2+} with DNAzyme influences the sensitivity of our sensing system. Thus, the cleavage time of Cu^{2+} with DNAzyme between 20 and 180 min was studied. As shown in Fig. 3B, the signal was increased with the cleavage time until 120 min. A longer cleavage time did not result in any obvious change. To save the assay, 120 min was selected as the cleavage time for Cu^{2+} with DNAzyme. Furthermore, the enzyme catalysis time also affects the system signal. Different catalysis times ranging from 5 to 50 min were investigated. As shown in Fig. 3C, the signal increased at a steady rate upon increasing the enzyme catalysis time until 40 min. Thus, a reaction time of 40 min was used in further steps.

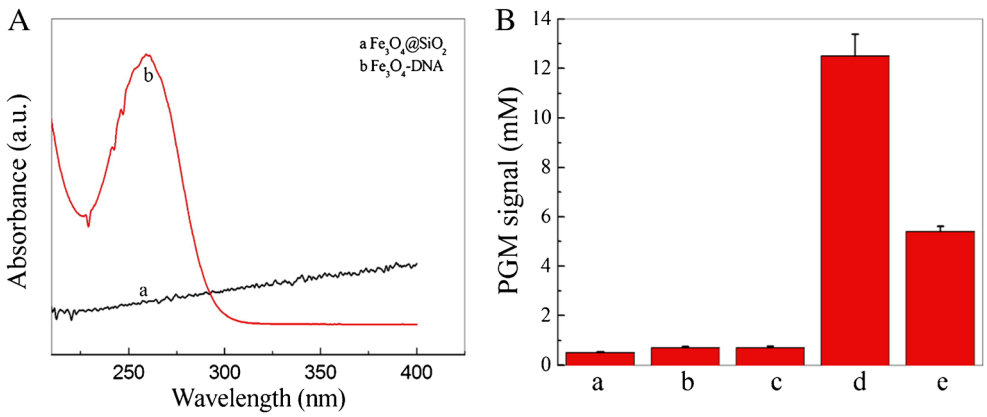

Fig. 2 **A** UV-Vis absorbance spectroscopy of Fe_3O_4@SiO_2 (a) and Fe_3O_4-DNA (b). **B** The PGM signal intensity under different conditions: (a) buffer solution, (b) Fe_3O_4-DNA, (c) magnetic sensing probe, (d) magnetic sensing probe in the presence of Cu^{2+}, (e) magnetic sensing probe in the presence of Cu^{2+} and PPi

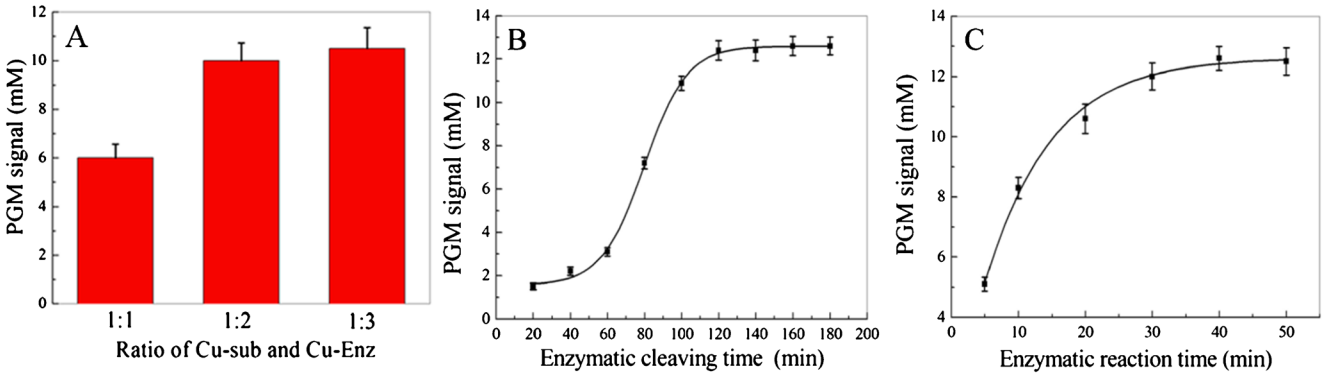

Fig. 3 The effect of the ratio of Cu-sub and Cu-Enz (**A**), the enzymatic cleaving time of Cu^{2+} with DNAzyme (**B**), and enzymatic catalysis time (**C**) on the PGM signal

Detection of Cu^{2+}

According to the above scheme, the concentration of Cu^{2+} was determined by the final concentration of released probes. Under the optimized conditions, the analytical performance of the proposed "off-on-off" sensor for Cu^{2+} was investigated. As shown in Fig. 4A, the PGM signals increased with the Cu^{2+} concentration. A linear relationship between the PGM signal and the logarithmic Cu^{2+} concentration was achieved in the range of 0.01–5 μM, as demonstrated in Fig. 4B. The linear equation for the PGM signal = 42.3811 + 5.1396lg$C_{[Cu2+]}$ (R = 0.9917). The detection limit was 10 nM. Compared with other reported references, our sensing system exhibits comparative sensitivity, as demonstrated in Table 1. Furthermore, the selectivity of this biosensor was investigated by replacing Cu^{2+} with other ions, such as Zn^{2+}, Pb^{2+}, Fe^{2+}, Mg^{2+}, Ca^{2+}, Ba^{2+}, and Cd^{2+}. No obvious changes in the PGM signal were achieved compared to that of Cu^{2+} at the same concentration, indicating the excellent selectivity of our biosensor. Subsequently, the stability of the sensing probe was evaluated by detecting the PGM signal over 14 days. The probe was prepared and stored in a refrigerator at 4 °C. After

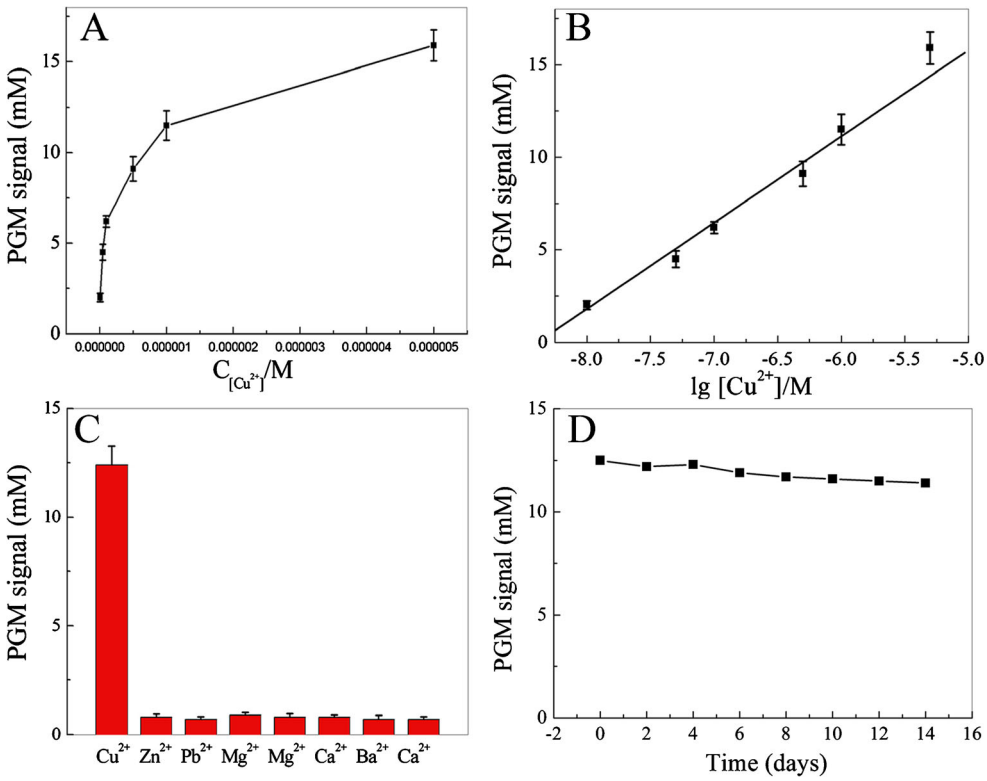

Fig. 4 **A** PGM signals of the sensor system with various concentrations of Cu^{2+}, **B** the corresponding linear relationship between the signal and the concentration of Cu^{2+} from 10 nM to 5 μM. **C** Selectivity of the sensor system for Cu^{2+} against Zn^{2+}, Pb^{2+}, Mg^{2+}, Ca^{2+}, Ba^{2+}, and Ca^{2+}. **D** Stability of the sensor system for Cu^{2+} determined by 14 days

Table 1 Comparison of our "off-on-off" sensor with reports from other references

Detection method	Linear range	Detection limit	Ref.
Chemiluminescence	0.002–9.0 μM	0.9 nM	[33]
Electrochemistry	0.1–30 μM	20 nM	[34]
Fluorescence	0.1–2 μM	57.8 nM	[1]
Lateral flow biosensor	–	10 nM	[35]
Dynamic light scattering	100 pM–2 nM	60 pM	[36]
Glucose meter	0.01–1 μM	10 nM	[28]
Glucose meter	0.01–10 μM	1 nM	[29]
Glucose meter	0.01–5 μM	10 nM	This work

Table 2 Comparison of our "off-on-off" sensor with reports from other references

Detection method	Linear range	Detection limit	Ref.
Fluorescence	0.5–8 μM	184 nM	[1]
Colorimetric	1–10 μM	700 nM	[9]
Fluorescence	–	10 nM	[37]
Fluorescence	0–5 μM	65.36 nM	[38]
Fluorescence	–	89 nM	[39]
Glucose meter	0.5–10 μM	500 nM	This work

2 weeks, the PGM signal of the biosensor kept about 91.2% of its initial value. The slight decrease in the signal response may be due to the gradual denature of SA and invertase. This is sufficient for the practical application of Cu^{2+} biosensors.

Detection of PPi

Furthermore, the feasibility of the sensing system for PPi detection with the support of Cu^{2+} was investigated. Figure 5A demonstrates the PGM signal of the sensor system for different concentrations of PPi in the presence of 5.0 μM Cu^{2+}. The PGM signals decrease with increasing PPi concentration. A linear relationship between the PGM signal and the PPi concentration is achieved in the range from 0.5 to 10 μM. The linear equation for the PGM signal = $15.0454 - 1.3163C_{[PPi]}$ ($R = 0.9920$). The detection limit was determined to be 500 nM. Compared with other reported references, our sensing system exhibits comparative sensitivity, as shown in Table 2. Furthermore, the selectivity of this biosensor was investigated by replacing PPi with other potential interferences including PO_4^{3-}, HPO_4^{2-}, $H_2PO_4^{-}$, HCO_3^{-}, CO_3^{2-}, SO_4^{2-}, and F^{-}. No obvious changes in the PGM signal were observed compared to that for PPi at the same concentration, indicating the excellent selectivity of our biosensor. This is sufficient for the practical application of PPi biosensors.

Detection of Cu^{2+} and PPi in real samples

To certify the potential application of our fabricated "off-on-off" biosensor for the determination of Cu^{2+}, tap water samples from Hangzhou Dianzi University with Cu^{2+} added were tested using the standard addition method. As demonstrated in Table 3, recoveries were obtained in the range of 96.8% and 116%. Moreover, human urine from Hangzhou Cancer Hospital was selected as an example for PPi detection. As demonstrated in Table 4, recoveries were obtained in the range of 96.6% and 109.6%, indicating excellent practical application ability in real analytical samples.

Conclusion

In summary, a portable, quantitative, and sequential monitoring system for copper ions and pyrophosphate based on a DNAzyme-Fe_3O_4 nanosystem and glucometer readout was fabricated. This "off-on-off" sensing system has the advantages of low cost, portability, and user friendliness. Satisfactory results were achieved for this biosensor for the detection of Cu^{2+} in real serum samples and PPi in human urine samples. Therefore, we anticipate that this biosensor has potential for application in clinical biological analysis and may lead to online, real-time sensing, and can be even employed for personal use in families.

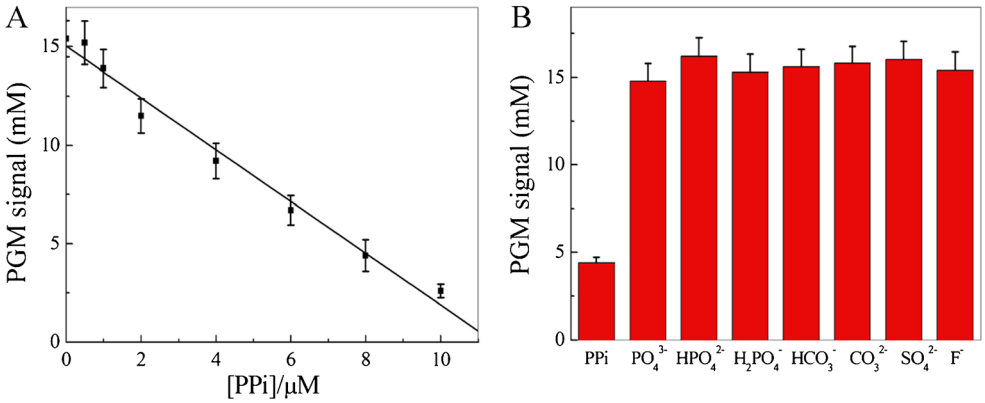

Fig. 5 **A** The corresponding linear relationship between the PGM signal and concentration of PPi from 0.5 to 10 μM. **B** Selectivity of the sensing system for PPi against other potential interferences

Table 3 Sensing system results obtained for real tap water samples

Sample number	Added (μM)	Found (μM)	Recovery (%)	RSD (%)
1	0.1	0.097	97.0	3.58
2	0.5	0.537	107.4	4.10
3	1	1.160	116.0	5.68

Table 4 Sensing system results obtained for human urine samples

Sample number	Added (μM)	Found (μM)	Recovery (%)	RSD (%)
1	1	1.008	100.8	2.12
2	5	4.830	96.6	3.98
3	10	10.960	109.6	5.76

Acknowledgements This study was financed by the Science and Technology Program of Zhejiang Province of China (LGC20H200001) and the Medical and Health Technology Development Program of Zhejiang province (2020KY727).

Declarations

Ethics approval The study was in accordance with the guidelines of the National Institute of Health, China, and approved by the Ethics Commission of Hangzhou Cancer Hospital.

Consent to participate All samples were collected with informed consent.

Conflict of interest The authors declare no competing interests.

References

1. Wang F, Zhang C, Xue Q, Li H, Xian Y. Label-free upconversion nanoparticles-based fluorescent probes for sequential sensing of Cu^{2+}, pyrophosphate and alkaline phosphatase activity. Biosens Bioelectron. 2018;95:21–6.
2. Tisato F, Marzano C, Porchia M, Pellei M, Santini C (2010) Copper in diseases and treatments, and copper-based anticancer strategies. Med Res Rev 30: 708–749.
3. Yuan L, Niu Y, Li R, Zheng L, Wang Y, Liu M, Xu G, Huang L, Xu Y. Molybdenum oxide quantum dots prepared via a one-step stirring strategy and their application as fluorescent probes for pyrophosphate sensing and efficient antibacterial materials. J Mater Chem B. 2018;6:3240–5.
4. Wang Z, Yu X, Li F, Kong F, Lv W, Wang W. Multiplexed ratiometric photoluminescent detection of pyrophosphate using anisotropic boron-doped nitrogen-rich carbon rugby ball-like nanodots. J Mater Chem B. 2018;6:1771–81.
5. Xu W, Zhu L, Shao X, Huang K, Luo YB. An electrochemical biosensor based on nucleic acids enzyme and nanochannels for detecting copper (II) ion. Biosens Bioelectron. 2018;120:168–74.
6. Wang D, Gao X, Li G, Xue T, Yang H, Xu H. Facile colorimetric assay of alkaline phosphatase activity using polydiacetylene liposomes with calcium ions and pyrophosphate. Sensor Actuat B: Chem. 2019;289:85–92.
7. Liu Y, Wu Y, Guo X, Wen Y, Yang H. Rapid and selective detection of trace Cu^{2+} by accumulation- reaction-based Raman spectroscopy. Sensor Actuat B: Chem. 2019;283:278–83.
8. Wang W, Zhou X, Wu S, Li S, Wu W, Xiong Z, Shi Q, Tian X, Yu Q. Reusable surface plasmon resonance sensor for rapid detection of Cu^{2+} based on modified-chitosan thin film as an active layer. Sensor Actuat B: Chem. 2019;286:59–67.
9. Zhang W, Liu S, Han L, Luo H, Li N. A ratiometric fluorescent and colorimetric dual-signal sensing platform based on N-doped carbon dots for selective and sensitive detection of copper (II) and pyrophosphate ion. Sensor Actuat B: Chem. 2019;283:215–21.
10. Wang H, Bai H, Wang Y, Gan T, Liu Y. Highly selective fluorimetric and colorimetric sensing of mercury(II) by exploiting the self-assembly-induced emission of 4-chlorothiophenol capped copper nanoclusters. Microchim Acta. 2020;187:185.
11. Wang H, Bai H, Mao A, Gan T, Liu Y. Poly(adenine)-templated fluorescent Au nanoclusters for the rapid and sensitive detection of melamine. Spectrochim Acta. 2019;219:375–81.
12. Wang H, Wang L, Huang K, Xu S, Wang H, Wang L, Liu Y. A highly sensitive and selective biosensing strategy for the detection of Pb^{2+} ions based on GR-5 DNAzyme functionalized AuNPs. New J Chem. 2013;37:2557–63.
13. Wang H, Mao A, Tao B, Zhang H, Liu Y. Fabrication of multiple molecular logic gates made of fluorescent DNA-templated Au nanoclusters. New J Chem. 2021;45:4195–201.
14. Hassan MM, Ranzoni A, Copper MA. A nanoparticle-based method for culture-free bacterial DNA enrichment from whole blood. Biosens Bioelectron. 2018;99:150–5.
15. Nayak S, Blumenfeld NR, Laksanasopin T, Sia SK. Point-of-care diagnostic: recent developments in a connected age. Anal Chem. 2017;89:102–23.
16. Montagnana M, Capito M, Lippi DG. Overview on self-monitoring of blood glucose. Clin Clim Acta. 2009;402:7–13.
17. Xiang Y, Lu Y. Using personal glucose meters and functional DNA sensors to quantify a variety of analytical targets. Nat Chem. 2011;3:697–703.
18. Shi H, Zheng J, Wang YX, Zhu S, Xiang Y, Zhu XL, Li GX. Point-of-care testing of protein biomarkers by integrating a personal glucose meter with a concatenated DNA amplifier. Sensor Actuat B-Chem. 2020;322:128659.
19. Liu R, He Y, Lan T, Zhang JJ. Installing CRISPR-Cas12a sensors in a portable glucose meter for point-of-care detection of analytes. Analyst. 2021;146(10):3114–20.
20. Fu P, Xu MJ, Xing S, Zhao Y, Zhao C. Dual cascade isothermal amplification reaction based glucometer sensors for point-of-care diagnostics of cancer-related microRNAs. Analyst. 2021;146(10):3242–50.
21. Zhang H, Chen GY, Qian ZM, Li WJ, Li CH, Hu YJ, Yang FQ. A portable personal glucose meter method for enzyme activity detection and inhibitory activity evaluation based on alkaline phosphatase-mediated reaction. Anal Bioanal Chem. 2021;413(9):2457–66.
22. Huang D, Shi ZW, Qian JJ, Bi K, Fang MJ, Xu ZN. A CRISPR-Cas12a-derived biosensor enabling portable personal glucose meter readout for quantitative detection of SARS-CoV-2. Biotechnol Bioeng. 2021;118(4):1587–96.
23. Yang YM, Wu TT, Xu LP, Zhang XJ. Portable detection of Staphylococcus aureus using personal glucose meter based on hybridization chain reaction strategy. Talanta. 2021;226:122132.
24. Zhang SB, Luan YX, Xiong MY, Zhang JJ, Lake R, Lu Y. DNAzyme amplified aptasensing platform for ochratoxin A detection using a personal glucose meter. ACS App Mater Inter. 2021;13(8):9472–81.

25. Kwon D, Lee H, Yoo H, Hwang J, Lee D, Jeon S. Facile method for enrofloxacin detection in milk using a personal glucose meter. Sensor Actuat B-Chem. 2018;254:935–9.
26. Zeng L, Gong J, Rong P, Liu C, Chen J. A portable and quantitative biosensor for cadmium detection glucometer as the point-of-use device. Talanta. 2019;198:412–6.
27. Zhang L, Gu C, Ma H, Zhu L, Wen J, Xu H, Liu H, Li L. Portable glucose meter: trends in techniques and its potential application in analysis. Anal Bioanal Chem. 2019;411:21–36.
28. Su J, Xu J, Chen Y, Xiang Y, Yuan R, Chai Y. Sensitive detection of copper (II) by a commercial glucometer using click chemistry. Biosens Bioelectron. 2013;45:219–22.
29. Ming J, Fan W, Jiang T, Wang Y, Lv Z. Portable and sensitive detection of copper(II) ion based on personal glucose meters and a ligation DNAzyme releasing strategy. Sensor Actuat B-Chem. 2017;240:1091–8.
30. Lu H, Zhou F, Shi D, Zhang X, Wang G. Portable aptamer biosensor of platelet-derived growth factor-BB using a personal glucose meter with triply amplified. Biosens Bioelectron. 2017;95:152–9.
31. Zhao Z, Long Y, Luo S, Wu W, Ma J. Preparation of magnetic mesoporous Fe_3O_4-Pd@TiO_2 photocatalyst for efficient selective reduction of aromatic cyanide. New J Chem. 2019;43:6294–302.
32. Wang L, Zhu F, Chen M, Xiong Y, Zhu Y, Xie S, Liu Q, Yang H, Chen X. Development of a "dual gates" locked, target-triggered nanodevice for point-of-care testing with a glucometer readout. ACS Sens. 2019;4(4):968–76.
33. Amjadi M, Abolghasemi-Fakhr Z. Gold nanostar-enhanced chemiluminescence probe for highly sensitive detection of Cu (II) ions. Sensor Actuat B-Chem. 2018;257:629–34.
34. Cheng B, Zhou L, Lu L, Liu J, Dong X, Xi F, Chen P. Simultaneous label-free and pretreatment-free detection of heavy metal ions in complex samples using electrodes decorated with vertically-ordered silica nanochannels. Sensor Actuat B-Chem. 2018;259:364–71.
35. Fang Z, Huang J, Lie P, Xiao Z, Ouyang C, Wu Q, Wu Y, Liu G, Zeng L. Lateral flow nucleic acid biosensor for Cu^{2+} detection in aqueous solution with high sensitivity and selectivity. Chem Commun. 2010;46:9043–5.
36. Miao X, Ling L, Cheng D, Shuai X. A highly sensitive sensor for Cu^{2+} with unmodified gold nanoparticles and DNAzyme by using the dynamic light scattering technique. Analyst. 2012;137:3064–9.
37. Li S, Cao D, Meng X, Hu Z, Li Z, Yuan C, Zhou T, Han X, Ma W. A novel fluorescent chemosensor based on coumarin and quinolinylbenzothiazole for sequential recognition of Cu^{2+} and PPi and its applicability in live cell imaging. Spectrochim Acta A. 2020;230:118022–9030.
38. Guo M, Dong P, Feng Y, Xi X, Shao R, Tian X, Zhang B, Zhu M, Meng X. A two-photon fluorescent probe for biological Cu (II) and PPi detection in aqueous solution and in vivo. Biosens Bioelectron. 2017;90:276–82.
39. Gao Y, Jiao Y, Zhang H, Lu W, Liu Y, Han H, Gong X, Li L, Shuang S, Dong. One-step synthesis of a dual-emitting carbon dot-based ratiometric fluorescent probe for the visual assay of Pb^{2+} and PPi and development of a paper sensor. J Mater Chem. 2019;7(36):5502–9.

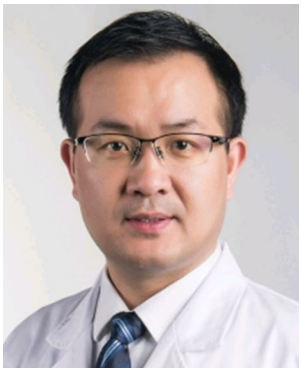

Chunchuan Gu is a docimaster in the Department of Clinical Laboratory, Hangzhou Cancer Hospital. His primary research interests focus on the application of nanomaterials in laboratory medical science.

Xiang Chen is head of Dongyang People's Hospital. His work is managing hospital quality, medical technology departments, and medical engineering departments. His current research focuses on nanomaterial-based biosensors.

Hongying Liu is a professor of Hangzhou Dianzi University. Her current research focuses on the synthesis of novel functionalized nanomaterials and exploration of their application in the biomedical area.